Check for updates

Gamma-aminobutyric acid-functionalized naphthalene diimide for aqueous organic flow batteries†

Mahsa Shahsavan, [iD] Cedrik Wiberg [iD] and Pekka Peljo [iD] *

An anionic gamma-aminobutyric acid-functionalized naphthalene diimide (GABA-NDI) was investigated for its possible application in flow batteries. A GABA-NDI/ferrocyanide flow battery was stable over 200 cycles and demonstrated an average coulombic efficiency of 99.96% and an excellent energy efficiency of 80.9% at 60 mA cm^{-2} while accessing 95% of the theoretical capacity of GABA-NDI. An increase in solubility and stability was achieved compared to previous studies.

A transition to using renewable energy sources is urgently needed to reduce fossil fuel consumption and provide societies with clean energy. However, due to the intermittent behavior of renewable energy resources, they cannot be utilized as the primary source for energy production unless the obtained energy is stored and fed into the grid on demand.[1] For this reason, energy storage systems, especially electrochemical systems, have become increasingly important during the last decade.[2]

One of the state-of-the-art electrochemical energy storage systems is flow batteries (FBs). FBs are safe and flexible systems that enable storing electrical energy decoupled from power in liquid electrolytes, *i.e.*, the charge capacity can be increased by increasing the volume of the electrolytes while the power can be increased by increasing the cell size and/or the number of the cells.[3] Present commercialized electrolytes for FBs are based on vanadium, making them too expensive for large-scale implementation.[4] Conversely, electrolytes using low-cost organic molecules based on abundant elements have the potential of lower capital costs than vanadium electrolytes.[5] Several properties and conditions govern the choice of organic molecules for aqueous organic flow batteries (AOFBs). Stability at all states of charge (SOC), high solubility in water, electrochemical reversibility, fast

kinetics, reduction potentials close to the water stability window, and cheap production costs are conditions that the chosen organic molecule should fulfill.[6] The structural tunability of organic molecules makes it feasible to synthesize molecules with the desired properties.[7] Organic molecule families such as quinones, viologens, pyridiniums, metallocenes, and 2,2,6,6-tetramethyl-piperidine *N*-oxyls (TEMPOs) have been widely studied and characterized due to their desirable characteristics that fit into the concept of AOFBs.[8] However, another attractive family of molecules that has recently gained attention as a possible candidate for FBs is 1,4,5,8-naphthalene diimides (NDIs).[9–11]

NDIs are molecules with two imide groups attached to a naphthalene core and have similarities with quinones. Like many quinones, NDIs are known to self-associate due to π–π stacking of their naphthalene core.[10] NDIs undergo a two-electron reduction reaction which is desirable as it can double the charge density of an electrolyte compared to molecules with single-electron reductions. The electrochemical properties of NDIs can be tuned by substitution on the core, and a suitable choice of the side chain on the imide nitrogen affects the solubility and can inhibit the self-association of the molecule.[10,11] NDIs have been studied for use in photovoltaics,[12] sensors,[13] semiconductors,[14] electrocatalysts,[15] and lithium-ion batteries,[16] while only a few papers have considered their use as redox-active material in AOFBs.[9,17]

The first demonstration of an NDI in a FB was reported by Medabalmi *et al.*[17] They coupled *N,N′*-bis(glycinyl) NDI (BNDI) with 4-OH-TEMPO across an anion exchange membrane (AEM) in a FB. Their system suffered from low solubility of the BNDI in KCl and NaCl as supporting electrolytes (30 mM and 40 mM, respectively). Although the use of 4-OH-TEMPO gave a high cell voltage, its crossover through the AEM led to a fast capacity fade in their battery. The second demonstration was recently done by Wiberg *et al.*, who demonstrated the performance of two different NDIs, *N,N′*-bis(dimethylaminopropyl)-NDI (2H-NDI) and *N,N′*-bis(dimethylaminopropyl)-2,6-bis(dimethylamino)-NDI (2DMA-NDI) coupled with bis((3-trimethylammonio)propyl) ferrocene dichloride (BTMAP-Fc) in FBs.[9] Their batteries displayed good

Research Group of Battery Materials and Technologies, Department of Mechanical and Materials Engineering, Faculty of Technology, University of Turku, 20014 Turku, Finland. E-mail: pekka.peljo@utu.fi

cyclability with high coulombic efficiencies, but they observed a gradual capacity fade in their battery that was more pronounced at higher concentrations of NDI. They stated that the source of their capacity loss was firstly because of the higher degree of self-association at higher concentrations of NDI and secondly because of the crossover of the BTMAP-Fc to the NDI side. Despite the higher solubility of NDI in this work compared to the BNDI, the use of AEM was necessary in the FB due to the positive charges on the 2H-NDI and 2DMA-NDI.

To solve the above problems regarding the use of NDI molecules in the FBs, the functionalization should provide the molecule with negative charges and high solubility. Herein, we synthesized a gamma-aminobutyric acid-functionalized naphthalene diimide (GABA-NDI) by a simple one-step method (Fig. S1, ESI†) and demonstrated its performance in a flow battery. To deprotonate GABA-NDI and make it water-soluble, the pH of the electrolyte was adjusted to 8.5. The presence of negative charges on GABA-NDI allows for it to be used in a flow battery with cation exchange membranes (CEM) that tend to have a higher conductivity and selectivity than the AEMs used in Wiberg et al. work.[9] The solubility of GABA-NDI was measured to be 587 mM in DI water (Fig. S18, ESI†) and approximately 250 mM in 1 M ammonium chloride (1 M NH_4Cl) which is higher than the solubility of BNDI (Table S7, ESI†).[17]

Cyclic Voltammograms (CV) of the synthesized GABA-NDI at pH 8.5 in 1 M NH_4Cl, show two stepwise redox reactions (Fig. 1). The redox potentials for the first and second redox reactions are −327 mV and −644 mV vs. Ag/AgCl (3 M KCl) (−115 mV and −432 mV vs. SHE), respectively. Like the previously studied NDI molecules by Wiberg et al., the reduction potential of GABA-NDI does not change by increasing the scan rate, indicating fast electron-transfer kinetics. A noticeable feature in the GABA-NDI CV is a small reduction peak located at approximately 80 mV after the first redox couple (−479 mV vs. Ag/AgCl (3M KCl)). According to the previous study, this peak could result from the dimerization of the molecule.[10] The scan rate-normalized CVs (Fig. S2, ESI†) show that the first reduction and the dimerization shoulder remain unchanged

Fig. 1 CV of 5 mM GABA-NDI in 1 M NH_4Cl at different scan rates.

while the reduction peak of the second reduction reaction is affected by the scan rate. We infer that this observation indicates a CE mechanism related to the dissociation of the dimer species.[10] At the beginning of the CV experiment, both monomer and dimer are present in the solution, and various combinations of electrochemical and chemical reactions can occur.[9] Therefore, for simplicity, we consider that the first redox reaction corresponds to the formation of GABA-NDI$^{-\bullet}$ and the second redox reaction to the formation of GABA-NDI^{2-}.

Rotating disk electrode measurements (RDE) were done to further investigate the system (Fig. S3, ESI†); however, as can be seen in the voltammograms, the limiting current of the first reduction is higher than that of the second reduction (Table S1, ESI†). Based on this observation, it is inferred that an appreciable degree of dimerization is observed for GABA-NDI. Using the Levich equation, an average diffusion coefficient of 3.7×10^{-6} cm^2 s^{-1} was calculated for the mixture of monomers and dimers in their oxidized forms (Fig. S4, ESI†). To test the cycling performance of GABA-NDI, a flow battery pairing GABA-NDI with ammonium ferrocyanide across a CEM (Selemion SX-053DK) was assembled. Ammonium ferrocyanide was synthesized using the previously reported procedure in the literature.[18] However, elemental analysis and ICP results showed that the ion-exchange procedure did not completely replace all sodium ions with ammonium (Tables S2–S4, ESI†), and the mixture of sodium ferrocyanide and ammonium ferrocyanide has nearly the same oxidation potential as that of the pure salts (Fig. S5, ESI†), and the material was used as obtained.

The studied batteries were built using 200 mM GABA-NDI in the negative electrolyte and a slight excess volume of 200 mM ammonium ferrocyanide in the positive electrolyte, giving an average voltage of 0.76 V (Fig. S6, ESI†). Three different batteries were studied in this paper. Two batteries were cycled in a nitrogen-filled glovebox and are referred to as buffered and unbuffered batteries. In the buffered battery, 1 M NH_4Cl and 0.5 M ammonium phosphate, and in the unbuffered battery, 1 M NH_4Cl were used as supporting electrolytes. A comparison between buffered and unbuffered supporting electrolytes was done as preliminary battery results showed that the pH on the negative electrolyte decreases after cycling GABA-NDI in the unbuffered supporting electrolyte. This is undesirable as GABA-NDI gradually starts to precipitate at lower pH values. Another battery was cycled outside the glove box and referred to as the air battery. In this battery, 1 M NH_4Cl was used as a supporting electrolyte. The battery was purged with nitrogen during cycling, but nonetheless, air infiltrated the system, and as such, it was studied to learn about the effect of oxygen on the NDI system.

The buffered and unbuffered batteries: battery performances are presented in (Fig. 2). Cycling at different current densities shows fast kinetics, as there is not much difference in the capacity utilization between 20 and 100 mA cm^{-2} (Fig. S7 and S8, ESI†). The buffered battery was cycled for 291 cycles (11 days), and the unbuffered battery cycled for 300 cycles (9 days). The accessed discharge capacities in buffered battery and unbuffered battery at 60 mA cm^{-2} are 95% and 97% of
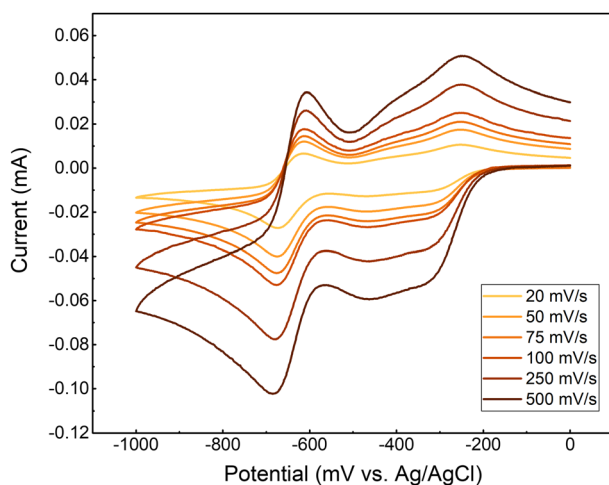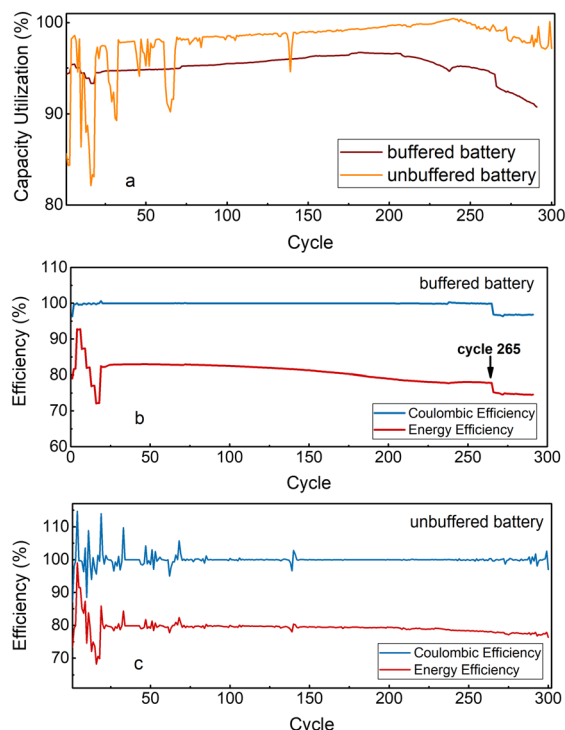
Fig. 2 (a) Capacity utilization of the batteries. (b) Buffered battery (negative electrolyte: 13 mL of 200 mM GABA-NDI, positive electrolyte: 30 mL of 200 mM ammonium ferrocyanide in buffer solution). (c) Unbuffered battery performance (negative electrolyte: 10 mL of 200 mM GABA-NDI, positive electrolyte: 30 mL of 200 mM ammonium ferrocyanide in 1 M NH$_4$Cl).

their respective theoretical values at the beginning of the cycling. An average coulombic efficiency of 99.96% and 99.98% is achieved for 244 cycles and 267 cycles at 60 mA cm^{-2} for the buffered battery and the unbuffered battery, respectively, while the energy efficiency of the buffered battery (80.9%) is marginally higher than the unbuffered battery (79.2%) at 60 mA cm^{-2} (Fig. 2b and c). In the buffered battery, a capacity increase of 0.012%/cycle was seen during the first 224 cycles at 60 mA cm^{-2}, after which the capacity started to decrease. After 265 cycles (240 hours), a minor leakage was detected in the system. After 291 cycles (263 hours), the inlet tubing disconnected from the cell due to a presumed pressure buildup leading to the electrolyte leakage, and the cycling was stopped afterward. Similar behavior was detected in the unbuffered battery, and an increase of 0.002%/cycle up to the 240th cycle was seen, followed by a gradual decrease until the end of cycling. From cycle 274 to the end, there was a slight voltage depression at the beginning of the voltage–time plots (Fig. S9, ESI†), and we observed that the inlet tube was clogged and the oxidized GABA-NDI was flowing more slowly. After first reduction the electrolyte was moving faster, indicating that the solubility of the oxidized GABA-NDI is slightly less than that of the reduced species. We speculate that the reason for the observed capacity increase in both batteries is due to a gradually increasing degree of dissociation of the NDI dimer, which would eventually reach an equilibrium for long-term cycling.[9] Post-mortem analysis of the negative electrolyte showed

that the pH had dropped to below 8 in both batteries (Table S5, ESI†). As mentioned before, a pH drop is detrimental to the cycling of GABA-NDI since the solubility of GABA-NDI decreases with decreasing pH. As a result, GABA-NDI precipitated on the carbon felt electrode (Fig. S12 and S17, ESI†) and the inner pressure of the battery increased and the inlet disconnected. The reason for the pH decrease in batteries could be the evaporation of ammonia from the solutions both during degassing of the electrolytes and during the cycling of the battery (Table S6, ESI†). Although the use of a buffer solution did not maintain the pH of the electrolyte during cycling, the buffered battery was more stable than the unbuffered battery (Fig. 2a). Cyclic voltammetry was done on the electrolytes after each battery finished cycling. CVs of GABA-NDI after the cycling in the buffered and unbuffered batteries look the same as before cycling; therefore, new redox-active species have not been formed during the cycling (Fig. S13, ESI†). No crossover of GABA-NDI to the positive electrolyte or vice versa was detected (Fig. S14 and S15, ESI†), and NMR results after cycling show no sign of degradation (Fig. S16, ESI†). Net water transfer from the negative side to the positive side due to unbalanced osmotic pressures between the electrolytes was observed. As a result, the concentration of the GABA-NDI increased during cycling and exceeded its solubility limit in the electrolyte. Additionally, permeation of sodium ions from the incompletely ion-exchanged ferrocyanide through the membrane could have led to the formation of sodium GABA-NDI which likely has a lower solubility than the ammonium form, as seen in the case of AQDS and ferrocyanide.[19] These phenomena led to the precipitation of active material on carbon felt and are proposed as the main mechanisms of capacity loss in the buffered and unbuffered battery.

The air battery: in the first cycle of the air battery, 83% of the theoretical capacity was accessed upon discharge; however, it lost 50% of its capacity after 5 cycles (2.45 h) (Fig. 3). After 50 cycles (7.2 h), the positive electrolyte was replaced with a new positive electrolyte, and the cycling continued. 80% of the theoretical capacity was accessed in cycle 51. At the end of the 56th cycle (after 2.75 h from cycle 51), only 50% of the initial capacity was accessed (Fig. 3). Although the solution was purged with nitrogen during the cycling, it seems even a small amount of oxygen that is already present in the solution or enters the solution during cycling is detrimental to the cycling
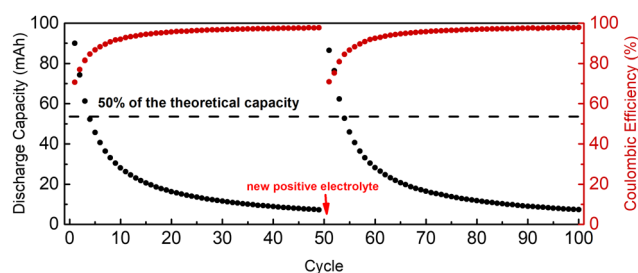

Fig. 3 Cycling of the air battery out of the glove box for 100 cycles (negative electrolyte: 10 mL of 200 mM GABA-NDI in 1 M NH$_4$Cl, positive electrolyte: 30 mL of 200 mM ammonium ferrocyanide in 1 M NH$_4$Cl).

of the GABA-NDI as oxygen oxidizes the reduced GABA-NDI, and this results in a charge imbalance between the SoC of the negative electrolyte and positive electrolyte, so further cycling is limited by the SoC of the negative electrolyte in every cycle.[20] After 100 cycles (14.4 h), the positive electrolyte was replaced again, and the battery was moved to the glovebox and cycled at 60 mA cm^{-2}. On the 101st cycle, 78% of the capacity was accessed, and the battery continuously lost its capacity, and by the 590th cycle (9 days), only half of the capacity could be achieved (Fig. S10, ESI†). After 590 cycles, 10 mL of 200 mM ammonium ferrocyanide in the supporting electrolyte was added to the positive electrolyte to determine if the capacity loss was due to an imbalance of the SoC between the negative electrolyte and the positive electrolyte. However, no change in capacity utilization was observed. The battery was cycled for 1000 cycles (13 days), followed by one day's rest, and then cycled again for 700 cycles (8 days), but the capacity did not recover (Fig. S11, ESI†). Although CVs and NMR do not show any sign of decomposition or crossover (Fig. S13–S16, ESI†), the irreversible capacity loss in this battery was likely related to the decomposition of GABA-NDI. Therefore, while cycling GABA-NDI, oxygen should be kept at a minimum level. Although the battery did not leak like the other two batteries, the same water transport effect was also seen in this battery (Fig. S11, ESI†) as in the previous batteries.

A comparison between the previously reported NDI molecules and the present work is presented in Tables S7 and S8 of ESI.†

In conclusion, we synthesized GABA-NDI, an NDI molecule bearing negative charges with higher solubility than the previous negatively charged NDI molecules in aqueous solutions, and coupled it with ammonium ferrocyanide in a flow battery. Three different batteries were studied, and the flow battery utilizing GABA-NDI in the buffered electrolyte showed better performance with a coulombic efficiency of 99.96% for 244 cycles and high energy efficiency of 80.9% at 60 mA cm^{-2}. The high energy efficiency of the studied batteries indicates fast kinetics and a low ohmic resistance compared to the previous studies. Despite the high dimerization observed in the CV and RDE, the battery performance at higher concentrations of the molecule did not seem to suffer as more than 95% of the capacity was accessed when cycling the battery galvanostatically at 60 mA cm^{-2}. The proposed mechanisms for the capacity loss were water transport, pH-drop due to the evaporation of ammonia, and lowered solubility due to formation of sodium GABA-NDI. However, before the mentioned mechanisms became dominant in the system, GABA-NDI showed good cycling stability, although a higher solubility would be needed for it to be feasible in industrial applications. The air sensitivity of the GABA-NDI was also studied. Oxygen oxidizes the reduced GABA-NDI, leading to a SoC imbalance and can possibly result in the decomposition of the molecule. The easy one-step synthesis makes GABA-NDI desirable for mass production at a low cost. The future study of our group is focused on providing the molecule with a higher solubility.

Conflicts of interest

A patent application has been filed with the application number PCT/SE2021/050814.

Notes and references

1 C. R. Dennison, H. Vrubel, V. Amstutz, P. Peljo, K. E. Toghill and H. H. Girault, *Chimia*, 2015, **69**, 753–758.
2 H. He, S. Tian, B. Tarroja, O. A. Ogunseitan, S. Samuelsen and J. M. Schoenung, *J. Clean. Prod.*, 2020, **269**, 121740.
3 A. Z. Weber, M. M. Mench, J. P. Meyers, P. N. Ross, J. T. Gostick and Q. Liu, *J. Appl. Electrochem.*, 2011, **41**, 1137–1164.
4 P. Leung, A. A. Shah, L. Sanz, C. Flox, J. R. Morante, Q. Xu, M. R. Mohamed, C. Ponce de León and F. C. Walsh, *J. Power Sources*, 2017, **360**, 243–283.
5 K. Wedege, E. Dražević, D. Konya and A. Bentien, *Sci. Rep.*, 2016, **6**, 1–13.
6 R. Chen, *ChemElectroChem*, 2019, **6**, 603–612.
7 Y. Ding and G. Yu, *Chem*, 2017, **3**, 917–919.
8 B. Hu, J. Luo, M. Hu, B. Yuan and T. L. Liu, *Angew. Chem.*, 2019, **131**, 16782–16789.
9 C. Wiberg, L. Evenäs, M. Busch and E. Ahlberg, *J. Electroanal. Chem.*, 2021, **896**, 115224.
10 C. Wiberg, F. Owusu, E. Wang and E. Ahlberg, *Energy Technol.*, 2019, **7**, 1–7.
11 C. Wiberg, M. Busch, L. Evenäs and E. Ahlberg, *Electrochim. Acta*, 2021, **367**, 137480.
12 M. Liu, P. Fan, Q. Hu, T. P. Russell and Y. Liu, *Angew. Chem., Int. Ed.*, 2020, **59**, 18131–18135.
13 S. Ali, M. A. Jameel, C. J. Harrison, A. Gupta, M. Shafiei and S. J. Langford, *Sens. Actuators, B.*, 2022, **351**, 130972.
14 N. Kumari, S. Naqvi, M. Ahuja, K. Bhardwaj and R. Kumar, *J. Mater. Sci.: Mater. Electron.*, 2020, **31**, 4310–4322.
15 S. Royuela, E. Martínez-Periñán, M. P. Arrieta, J. I. Martínez, M. M. Ramos, F. Zamora, E. Lorenzo and J. L. Segura, *Chem. Commun.*, 2020, **56**, 1267–1270.
16 A. E. Lakraychi, K. Fahsi, L. Aymard, P. Poizot, F. Dolhem and J. P. Bonnet, *Electrochem. commun.*, 2017, **76**, 47–50.
17 V. Medabalmi, M. Sundararajan, V. Singh, M. H. Baik and H. R. Byon, *J. Mater. Chem. A*, 2020, **8**, 11218–11223.
18 J. Luo, B. Hu, C. Debruler, Y. Bi, Y. Zhao, B. Yuan, M. Hu, W. Wu and T. L. Liu, *Joule*, 2019, **3**, 149–163.
19 B. Hu, J. Luo, M. Hu, B. Yuan and T. L. Liu, *Angew. Chem.*, 2019, **131**, 16782–16789.
20 T. Páez, A. Martínez-Cuezva, R. Marcilla, J. Palma and E. Ventosa, *J. Power Sources*, 2021, **512**, 10–15.